Synergic kinetics and strategies for enhanced photopolymerizations for 3D-printing and additive manufacturing - A Critical Review

. **Jui-Teng Lin *[1], Jacques Lalevee[2], Da-Chun Cheng[3]***

. [1] New Vision Inc., 10F, No. 55, Sect.3, Xinbei Blvd, Xinzhuang, New Taipei City, Taiwan, ROC; jtlin55@gmail.com

. [2] Université de Haute-Alsace, CNRS, IS2M UMR 7361, F-68100 Mulhouse, France; jacques.lalevee@uha.fr

. [3] Department of of Biomedical Imaging and Radiological Science, China Medical University, Taichong, Taiwan, ROC, dccheng@mail.cmu.edu.tw

.

. * Correspondence: jtlin55@gmail.com ; and dccheng@mail.cmu.edu.tw

Abstract: *The synergic features and enhancing strategies for various photopolymerization systems are reviewed by kinetic schemes and the associated measurements. The important topics include: (i) photo crosslinking of corneas for the treatmnet of corneal deseases using UVA-light (365 nm) light and riboflavin as the photosensitizer; (ii) synergic effects by a dual-function enhancer in a 3-initiator system; (iii) synergic effects by a 3-initiator C/B/A system, having an electron-transfer and oxygen-mediated energy-transfer pathways; (iv) copper-complex (G1) photoredox catalyst in G1/Iod/NVK systems for free radiical (FRP) and cationic photopolymeriation (CP); (v) radical-mediated thiol-ene (TE) photopolymerizations; (vi) superbase photogenerator based-catalyzed thiol–acrylate Michael (TM) addition reaction; and the combined system of TE and TM usinghual wavelength; (vii) dual-wavelength (UV and blue) controlled photopolymerization confinement (PC); (viii) dual-wavelength (UV and red) selectively controlled 3D printing; and (ix) 3-wavelength selectively controlled in 3D printing and additive manufacturing (AM). With minimum mathematics, we present (for the first time), the synergic features and enhancing strategies for various systems of multi-commponents, initiators, monomers, and under one- two- and there-wavelength light. Therefore, this Review provides not only the bridging between modeling and measurements, but also guidances for further experimental studies and new applications in 3D printings and additive manufacturing (AM), based on the innovative concepts (kinetics/schemes).*

Keywords: 3D printings; additive manufacturing; polymerization kinetics; photoredox; monomer conversion; synergic effects; cationic ; free radical. UV visible light.

---

1. Introduction

The advantages of photopolymerization over the conventional thermal-initiated polymerization include the following: (i) fast and controllable reaction rates, (ii) spatial and temporal control over the formation of the material, without the need for high temperatures or harsh conditions, (iii) synergic effects and enhancement are available by using co-initiators or catalyic complexes [1,2]. Photopolymerizations using various light with wavelength in UV, visible and near IR have been studied for both industrial and medical applications. Variety of photoresponsive materials such as conjugated polymers have been reported for additive manufacturing (AM) and recently for 3D and 4 D bioprinting [3-11]. Both spatial and temporal controlled 3D processes were reported using single and multiple wavelength lights. For 3D photo printings, the key factors include polymerization depth, resolution precision and speed, in which the monomer conversion efficacy could be improved by various strategies [12-18]. They include (i) thiol–Michael/acrylate hybrid, epoxy/acrylate curable resins, thiol–acrylate/thiol–acetoacetate thermosets, and thiol–ene/epoxy-based polymers [12-14]; (ii)the use of novel materials as enhancers or co initiators in both single and multiple components

[15-17]; (iii) two stage polymerization under two wavelengths to eliminate the oxygen inhibition effects [17-19].

UV light (at 365 nm) have been commonly used in most type-I photoinitiators for the photopolymerization of (meth)acrylate monomers [1-3]. However, the UV wavelength suffers the disadvantages of being unsafe to skin and eyes, small penetration depth and larger light scattering in tissues [1,2]. Camphorquinone (CQ), due to its good visible absorption properties, is the most common type-II free radical photopolymerization of (meth-) acrylates under blue light [15,20]. The classical diaryliodonium salts, such as diaryliodonium, suffer low solubility in monomers and formation of side products due to the release of HF. To overcome this drawback, Kirschner et al. [15] recently reported a new counter anion-free and fluoride-free aryliodonium ylides (AY) to avoid the formation of HF and to enhance their solubility. They reported (CQ)/amine/AY as a new and efficient PI system for the polymerization of methacrylates under air and blue light (477 nm) irradiation. Kirschner et al. [15] also reported the chemical mechanisms involved in the presence of various AY and amines which lead to additional reactions and initiating radicals for improved conversion efficacy.

In comparison, near-infrared (NIR) light offers advantages of safer, less light diffusion and scattering, and deeper penetration into the materials. Thus, the curing of a thick and filled material can be potentially enhanced compared to curing with UV or visible light. However, the use of NIR photoinitiating systems such as cyanine is often associated with a low reactivity and requires a high light intensity. Phthalocyanines, conjugated macrocycles, have been used as commercial pigments and dyes having a high molar absorptivity coefficient in the red and NIR wavelength of 650-810 nm. Efficient polymerization conversions using NIR photoinitiation by cyanine/iodonium salt couples are reported by Schmitz et al [16]. Recently, Bonardi et al [17] reported the first three-initiator system for high performance NIR (785 nm) photopolymerization of thick methacrylates, in which a dual-function enhancer (phosphine) to prevent oxygen inhibition, and to regenerate the PS upon irradiation, in which a stable radical is coupled with the enhancer. The 3-initiator system with a dye as a photosensitizer absorbing in the NIR range, an iodonium salt (as an initiator), and a phosphine (as a co-initiator) was reported, in which the phosphine is used to reduce oxygen inhibition (OIH) during the free radical polymerization of (meth)acrylate monomers [17,18].

Oxygen-inhibition plays a critical role specially for optically-thin polymers. Various strategies to reduce oxygen inhibition in photoinduced polymerization have been proposed such as : (i) using a higher photoinitiator concentration; (ii) using a higher light dose or intensity, (iii) using co-initiators, (iv) addition of oxygen scavengers, and (v) working in an inert environment [19]. Besides the above methods, chemical mechanisms were also reported, such as the thiol-ene and thiol-acrylate-Michael systems which are insensitive to oxygen [12-14]. Additive enhancer-monomer were proposed to improve the curing (crosslink) efficacy by either reducing the oxygen inhibition effect by stable-monomer, or increase the lifetime of radicals in clinical applications. Dual-wavelength (red and UV) photopolymerization was also reported, in which pre-irradiation of the red light eliminated the oxygen inhibition effect and thus enhanced the conversion efficacy of the UV light [10, 18,19].

Example of blue and UV dual-wavelength system (without the red-light) for enhanced conversion by reducing the oxygen inhibition was reported by de Beer et al [8] and van der Laan et al [9], in which a blue (470 nm) and a UV (365 nm) light were used for the photopolymerization of methacrylate formulated with camphorquinone (CQ) and ethyl 4-(dimethylamino)benzoate (EDAB), where CQ is the blue-light active initiator (A), butyl nitrite (BN) is the UV-activated initiator (B), and EDAB is a co-initiator (or donor D). Lin et al [20] reported the theoretical modeling for the above described 2-wavelength system.

Example of 2-wavelength (red and UV) system (without the blue-light) for 3D printing was reported by Childress et al [10], in which a monomer of ethyl ether acrylate (DEGEEA) mixed by zinc 2,9,16,23-tetra-tert-butyl-29H,31H-phthalocyanine (ZnTTP) as an initiator under a UV-light, where ZnTTP/DEGEEA has distinct absorption peak at UV-365 nm and red-635 nm, respectively, and thus it can be independently excited by a UV and a red light, respectively. Lin et al [21] reported the theoretical modeling for the above described 2-wavelength system. The novel strategy using 3–

wavelength of uv, blue and red lights was recently proposed by Lin et al [22] theoretically for future experimental studies.

Multicomponent photoinitiating systems using dye as visible light absorbing compounds have also attracted many attention for visible light curing [23-27]. These systems often based on dye/iodonium salt/amine combinations have often the great advantages to generate simultaneously initiating radicals and cations species [25]. Therefore, these latter sytems can advantageously initiate both free radical and/or cationic polymerization processes. Three-component (Coum/NPG/Iod) photoinitiating systems for the free radical photopolymerization of (meth)acrylates using the new synthesized set of in-silico developed coumarin derivatives was investigated by Abdallah et al [25,26], which offers two distinct strategies: a photooxidation approach based on an iodonium salt and a photoreduction approach based on an amine under visible LED as source of irradiation.

Recently, another 3-component of G1/Iod/NVK, and G1/Iod/EPOXY photoinitiating systems were invested by Mokbel et al [28,29] using copper complex (G1), in which the co-initiators/additives Iod/NVK have dual functions of: (i) regeneration of photoinitiator, and (ii) generation of extra radicals. The synergic effects lead to higher conversion of free radical polymerization (FRP) and cationic polymerization (CP). The kinetics of copper complex photoredox catalyst including the roles of oxygen, thickness, and optimal concentration for radical/cationic hybrid photopolymerization was reported by Lin et al [30].

Table 1 summarizes various reported enhancing strategies for photopolymerization including one component (or monomer) and one-wavelength, two-component and one, two and three-wavelength [9-12,14,19-21] and three-component, one-wavelength system [26-31]. We note that all these systems have been theoretically and experimentally studied, except the 3–wavelength systems which was recently proposed theoretically by Lin et al [22].

Table 1. Summary of enhancing strategies for photopolymerization

System	light	Enhancer	References
one-component		co-initiators	
	blue (477 nm)	CQ/EDB/AY	Kirschner et al. [15]
	UV (365 nm)	BP/EDB/Iod	Liu et al [23]
	green (532 nm)	CQ/rose-Bengal	Wertheimer et al [31]
	NIR (785 nm)	phosphine/Iod	Bonardi et al [17].
			Chiu et al [18]
two-component		co-monomers	
	UV (365 nm)	thiol–Vinyl (Michael)	Claudino et al [12]
		thiol–Ene	Chen et al [14]
	dual (365 + 660 nm)	DEGEEA/ZnTTP	van der Laan et al [9]
			Childress [10]
			Lin et al [19]
	Dual (365 + 430 nm)	DEGEEA/ZnTTP	Scott et al [11]
			Lin et al [20,21]
	3-wave (365,430, 660)	DEGEEA/ZnTTP	Lin et al [22]
three-component	UV (365 nm)	Thiol BMP/EVS/BA	Huang et al [13]
	UV (365 nm)	PI/EDB/Iod	Liu et al [24]
	UV (405 nm)	Meth/Iod/NPG	Abdallah et al [26,27]
	UV (405 nm)	G1/Iod/NVK	Mokbel et al [29,30],
			Lin et al [31]

* CQ=Camphorquinone, AY=aryliodonium ylides, EDB=ethyl 4-(dimethylamino)benzoate; Iod= (4-*tert*-butylphenyl)iodonium hexafluorophosphate; BP=benzophenone; DEGEEA=ethyl ether acrylate, ZnTTP=zinc

2,9,16,23-tetra-tert-butyl-29H,31H-phthalocyanine; BMP=1-butyl mercaptopropionate; EVS=ethyl vinyl sulfone; BA= 1-butyl acrylate. G1=copper complex, NVK= *N*-vinylcarbazole.

This article will review, for the first time, the following kinetics and the synergic features of various systems (as summarized in Table 1), in which measured data are analyzed by modelings.

(1) Photo crosslinking of corneas for the treatmnet of corneal deseases using UVA-light (365 nm) light and riboflavin as the photosensitizer.
(2) Synergic effects by a dual-function enhancer in a 3-initiator system (one-monimer).
(3) Synergic effects by a 3-initiator C/B/A system, having an electron-transfer and oxygen-mediated energy-transfer pathways for free radical (FRP) and cationic photopolymerization (CP).
(4) Copper-complex (G1) photoredox catalyst in G1/Iod/NVK systems for FRP and CP.
(5) Radical-mediated thiol-ene (TE) photopolymerizations.
(6) Superbase photogenerator based-catalyzed thiol–acrylate Michael (TM) addition reaction. and the combined system of TE and TM.
(7) Dual-wavelength (UV and blue) controlled photopolymerization confinement (PC)
(8) Dual-wavelength (UV and red) selectively controlled 3D printing
(9) 3-wavelength selectively controlled in 3D printing and additive manufacturing (AM).

With minimum mathematics, we present (for the first time), the synergic features and enhancing strategies for various systems of multi-commponents, co-initiators, co-monomers, and under one- two- and three-wavelength light. Therefore, this Review provides not only the bridging between modeling and measurements, but also guidances for further experimental studies and new applications, based on the innovative concepts (kinetics/schemes) published in the recent few years.

2. Kinetic systems and Discussions

2.1. Photo crosslinking of corneas

Figure 1 shows the schematics of a one-component photochemical pathways: (i) radical-mediated, and (ii) oxygen-mediated pathway. A typical example is applying riboflavin solution (photoinitiation agent) to the cornea, which is irradiated by a UVA light (at 365 nm) for a procedure called corneal collagen crosslinking (CXL) [32-34]. Similar to the procedure of CXL is a type-II procedure for anti-cancer, in which cancer cells are killed by the oxygen singlet radical [35-37]. Synergic therapy combining photodynamic therapy (PDT) and photothermal therapy (PTT) are also studied recently [38-40].

Greater details of Figure 1 are shown in Figure 2 for the kinetics of a photosensitizer (PS), monomer-A, with three reactive radicals, R’ and R and singlet-oxygen. The two pathways are described as follows. The ground state PS molecules (C) are excited by the UV light to its singlet excited state (C_1), which could be relaxed to its ground state or to a triplet excited state (T*). In type-I process, T* could interact directly with the substrate [A] to produce the first-radical (R’) which could produce (by chain reaction) a second-radical (R), which could interact with the ground state oxygen [O_2] or with the first-radical (R'), or te bimolecular termination (R^2). For a type-II process, T* interacts with [O_2] to form oxygen singlet [$^1O_2$] which could relax to its groundstate [O_2], or interacts with the substrate [A]. For example, in a CXL procedure, A (monomer) is the corneal stroma matrix, C is riboflavin solution.

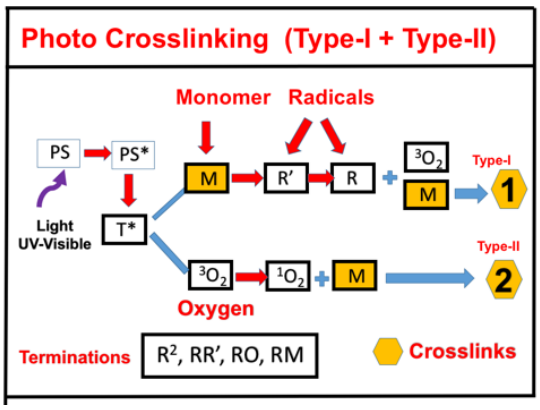

Figure 1. Schematics of photochemical pathways: (i) radical-mediated, (ii) and oxygen-mediated pathway; where PS is the ground state photosensitizer, having an excited state (PS*) and triplet state (T*) which interacts with the substrate A to form radicals R′ and R. It also may interact with the oxygen to form singlet oxygen. After Lin [33], Ophthalmology Research, 2017;7:1-8.

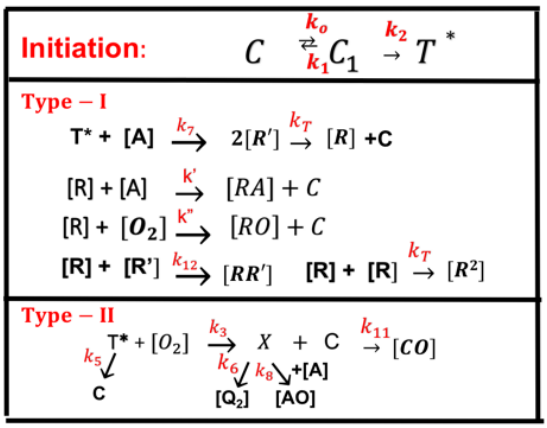

Figure 2. Schematics of photochemical pathways of 1-monomer system. The ground state PS (C) is excited by a UV-light to its singlet excited state (C_1), which could be relaxed to its ground state or to a triplet excited state (T*). In type-I process, T* could interact directly with the monomer [A] to generate free radical (R′) by recombination. The radical R could interact with [A] for crosslinking, or oxygen [O_2], or terminated by coupling with R′, or bimolecular recombination ($2R^2$). For type-II process, T* interacts with [O_2] to form oxygen singlet [$^1O_2$] (X), which could relax to its oxygen [O_2], or interacts with [A] for crosslinking, or coupling with C. All rate constants are shown in reds next to arrows. After Lin [34], Ophthalmology Research, 2017;7:1-8.

2.2. Synergic effects of a dual-function enhancer (3-initiator system)

There are many strategies for improved photopolymerization such as the reduction of oxygen inhibition effects (OIH) and using co-initiators (or enhancers). Three-component system using the phosphine to reduce the OIH effects during the free radical polymerization of (meth)acrylate monomers has been reported [17,18]. Figure 3 shows the kinetic scheme of a 3-initiator system, [C], [A] and [B], in the presence of oxygen, using an enhancer-initiator [B]. Under a near-infrared (NIR) light exposure, the initiator dye (C) is exited to its excited triplet-excited state, given by C*, which could react with initiator [A] to produce active radical (R) or react with co-initiator [B]; where dye [C] is regenerated in both reactions. The coupling of radical [R] and oxygen [O_2] produces a peroxyl radical [ROO°], which is too stable for the polymerization to proceed. Therefore, an enhancer-initiator [B] is required to create less stable radical [RO] for extra crosslinks of the monomer, [M].

We note that the initiator [B] plays a dual-function of: (i) regeneration of dye [C], and (ii) reducing OIH and generating an extra active radical [RO] for improved conversion. Without the dual-function enhancer [B], OIH reduces the radical [R] and the conversion efficacy, in which an induction time is defined for the delayed rising of the conversion curve [18].

Example of above system was reported by Bonardi et al [17], in a 3-component system of C/B/A, in which [C]= IR-140 borate, [B] = 4-(Diphenylphosphino) benzoic acid (4-dppba), and [A] = iodonium salt $Ar_2I^+PF_6^-$, with initial concentration of [0.1/2.0/3.0] wt%, and mixed in a monomer [M]=methacrylate.

Several unique features for the conversion are demonstrated [18]. For examples, reverse trends (roles) are found in: (i) the light intensity and enhancer concentration, and (ii) the coupling rate constants of radical-oxygen and radical-monomer. The monomer conversion is an increasing function of enhancer, oxygen concentration, and the light intensity. However, they have significantly different steady state feature. Lin et al [17] reported the steady-state conversion increases from 10% without the enhancer (with enhancer concentration $[B]_0$=0) to (30%, 50%, 80%) for $[B]_0$=(0.5, 1.0, 2.0)%.

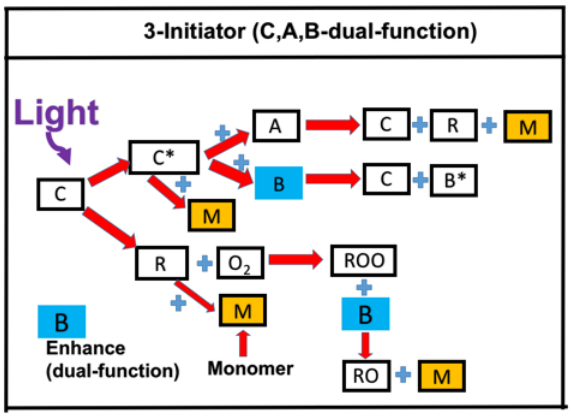

Figure 3. Schematics of photochemical mechanisms in a 3-initiator (C/B/A) system under an near-infrared light; in which the initiator dye (C) is excited to its excited triplet state C*, which could react with [A] to regenerate [C], and produce active radical (R). R could initiate crosslink of the monomer [M] or react with oxygen producing a radical [ROO], which reacts with [B] to produce radical [RO] causing extra crosslink of [M]. After Chiu et al [18], IEEE Access, 2020, 8, 83465-83471.

2.3. Synergic effects of a 3-initiator enhanced C/B/A system

Figure 4 shows the schematics of photochemical pathways in a 3-initiator C/B/A system [20]. Example of Figure 4, is shown by the reported (CQ)/amine/AY system of Kirschner et al. [15], corresponding to our C/B/A system, where AY (aryliodonium ylides) is our [A], and amine (our [B], the enhancer), could be Ethyl-4-(dimethylamino)benzoate (EDB) or 4-(dimethylamino)benzonitrile (DMABN) additives in multicomponent PI systems. The aryl radicals R) were generated through an electron transfer between CQ and the AY. In the presence of amine (EDB, or DMABN), additional reactions were expected [15] leading additional initiating radicals (R), via the interaction of excited molecule (CQ-H*) with AY. The free radical initiates the photopolymerization of the monomer, (meth-)acrylates, besides the oxygen-mediated photopolymerization.

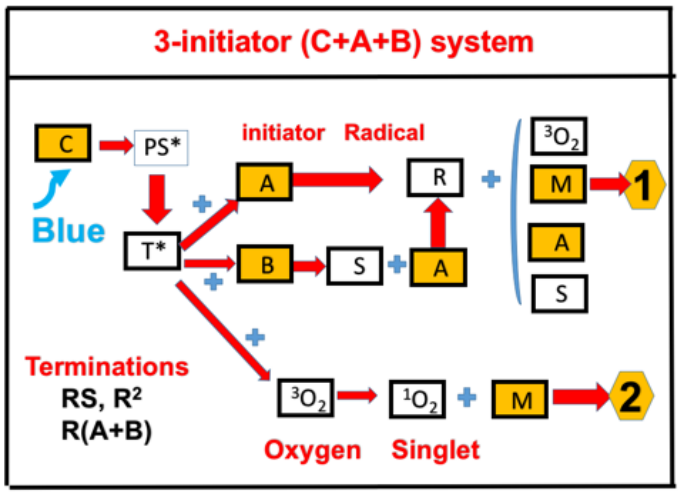

Figure 4. Schematics of photochemical pathways in a 3-initiator C/B/A system, having an electron-transfer pathway-1, and an oxygen-mediated energy-transfer pathway-2. After Lin et al [20], J Polymer Research, 2021, 28:2.

The measured system reported by Kirschner et al [15] showed that conversion could be improved by higher concentration of the additive initiators and the kinetic rate constants. These features are consistent with our modeling. Competing mechanisms between the reduction of conversion due to light intensity reduced (in thick polymer) and the reduction of oxygen inhibition (higher conversion) were analyzed in thick polymer [20]. The optimal conditions are governed by the product function of the light intensity and main initiator concentration (C_0), in which conversion efficacy has a normal-trend proportional to C_0I_0, for the transient-state, but a reversed-trend for the steady-state. Strategies for improved conversion include: increasing the photoinitiator concentration, the light dose and intensity, addition of oxygen scavengers and use of multiple photoinitiators. In the CQ/DMABN/AY system, Kirschner et al [15] reported that higher AY (from 0% to 0.75%) leads to higher conversion (from about 40% to 60%).

2.4. Synergic effects in a 3-initiator (A/B/C) system for FRP and CP

Figure 5 shows the schematics of a 3-initiator system, (A/B/C), with electron-transfer and oxygen-mediated energy-transfer pathways. A specific system was reported by Liu et al [23], where [A] is benzophenone (BP) photoinitiator, co-initiator [B] is ethyl 4-(dimethylamino)benzoate (EDB), and [C] is (4-tert-butylphenyl)iodonium hexafluorophosphate (Iod). Under a UV (365 nm) LED irradiation, [A] transforms from ground state (PI) to excited triple state ^{1,3}PI. For BP alone, PI-H' (or R) and PI(-H)$^{\cdot}$ (or R') are the active species for FRP. In the presence of EDB, extra radical PI-H' is produced and could couple with [C] to produce aryl radical Ar' and cation PI' which lead to free radical (FRP) and cationic photopolymerization (CP), respectively. Associated with the photolysis of BPC1/Iod and BPC1/EDB/Iod, the photoredox catalytic cycle was proposed in three-component PI/EDB/Iod system [23,24]. The regeneration of PI speeds up the photopolymerization and slows down the consumption of PI in the photolysis experiments. Trimethylolpropane triacrylate (TMPTA) and (3,4- epoxycyclohexane)methyl 3,4-epoxycyclohexylcarboxylate (EPOX) were used as benchmark monomers for FRP and CP, respectively.

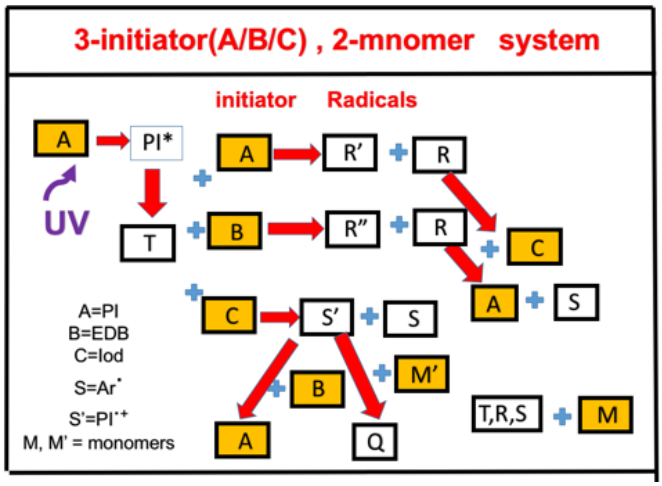

Figure 5. The schematics of a 3-initiator system, (A/B/C), where A is the ground state initiator, having a first excited state PI*, and a triplet state T, which interacts with initiator [A] and [B] to produce radical R; and interacts with initiator [C] to produce radical S, in which the coupling of the radical R with [C] and S′ with [B] could lead to the regeneration of [A]. After Chen et al [24], Res Med Eng Sci. 2019, 8(2):853-860.

The co-initiators/additives B and C have dual functions of : (i) regeneration of photoinitiator A and (ii) generation of extra radicals. The synergic effects lead to higher conversion of free radical polymerization (FRP) and cationic polymerization (CP) in consistent with the measured work of Liu et al [24]. However, there are other theoretically predicted new features (findings) which are either not identified or explored experimentally, including: (i) co-initiator [C] always enhances both FRP and CP conversions, whereas co-initiator [B] leads to more efficient FRP, but it also reduces CP; (ii) The FRP conversion is proportional to the square-root of (bIg)([A]+[B]+[C]), whereas CP conversion is proportional to the linear power of (bIg)[A][C]/[B], where I is the light intensity, and [A], [B] [C[are the initial concentration of the co-initiators, and b, g are rate constants; (iii) The dominant polymerization is FRP or CP depending on the relative concentration of [A][C] and [B] and the rate constants which define the amount of radicals; (iv) the steady state CP conversion profile is independent to the light intensity, whereas higher light intensity reaches a lower steady state value for the profile of FRP. The specific systems analyzed are: benzophenone derivatives (A) ethyl 4-(dimethylamino)benzoate (B), and (4-tert-butylphenyl)iodonium hexafluorophosphate (C) under a UV (365 nm) LED irradiation; and two monomers of trimethylolpropane triacrylate (TMPTA, for FRP) and (3,4- epoxycyclohexane)methyl 3,4-epoxycyclohexylcarboxylate (EPOX, for CP).

We note that Figure 5 is more general than the Scheme proposed by Liu et al [23], which ignored the coupling of $PI^{\cdot+}$ and epoxy monomer producing a propagating cation (Q) which could be terminated by [B] as cationic polymerizations were not experimently carried out in presence of B due to its inhibitor effect. Furthermore, the measured data of Liu et al [23] for the case of CP was limited to two initiators of [A] and [C], although 3-initiator systems of [A]/[B]/[C] was studied in FRP. The modeled system of Chen et al [24] in Figure 5 and the associated kinetic equations include 3-initiator for both FRP and CP.

2.5. Copper-complex (G1) photoredox catalyst in G1/Iod/NVK systems

Figure 6 shows the schematics of a 3-initiator system, (A/B/N) for copper-complex (G1) photoredox catalyst systems for FRP and CP [28-31]. A specific measured system of G1/Iod/NVK related to Figure 6 was reported by Mokbel et al [28] with a proposed scheme (shown by Figure 7), in which the G1 in combination with iodonium salt (Iod), (oxidizing agent) generates the radical species through an electron transfer reaction. A propagation system containing the N-vinylcarbazole

(NVK) additive leads to simultaneous regeneration of G1 and the formation of highly reactive cations (Ph- NVK+), which can very efficiently initiate the CP conversion [28]. Figure 8 shows the 3D-photopolymerization experiments using LED projector @405 nm [28].

The general conversion features of a 3-initiator system (A/B/N), based on proposed mechanism of Mokbel et al [29,30], for both FRP of acrylates and the free radical promoted CP of epoxides using copper complex as the initiator are summarized as follows based on the modleing of Lin et al [30]. Higher FRP and CP conversion can be achieved by co-initiators concentration [B] and [N], via the dual function of (i) regeneration [A], and (ii) generation of extra radicals S' and S. The FRP and CP conversion is proportional to, respectively, the nonlinear and linear power of bI[A][B], where b and I are the absorption coefficient and the light intensity, respectively. System in air has lower conversion than in laminate due to the oxygen inhibition effects. For thick samples (with thickness z), there is an optimal concentration [A*] which is inverse proportional (bzI), in contrast with very thin sample, in which the conversion is an increasing function of [A] and [B]. The unique feature of dark polymerization in CP conversion enables the polymerization to continue in living mode, in contrasts with that of the radical-mediated pathway in most conventional FRP.

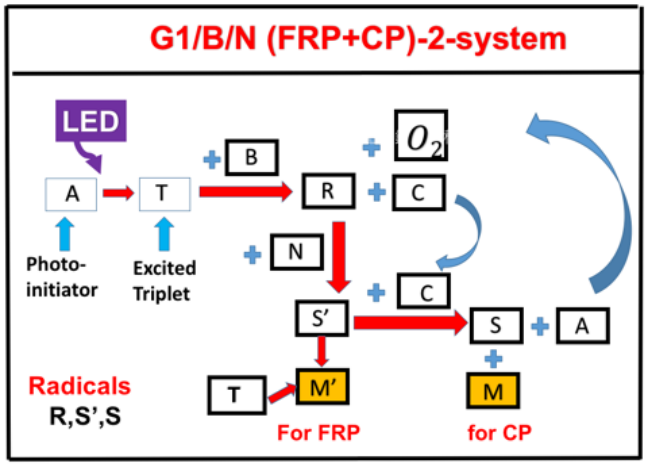

Figure 6. The schematics of a 3-initiator system, (A/B/N), where A is the ground state of initiator-A, having an excited triplet state T, which interacts with co-initiator [B] to produce radical R and oxodized-A (or [C]); R interacts with co-initiator (or additive) N to produce radical S', which couples with [C] to produce another radical S and lead to the regeneration of [A]. Monomer M' and M coupled with radicals S' and S for FRP and CP conversion, respectively. After Lin et al [30], Polymers (2021, in press).

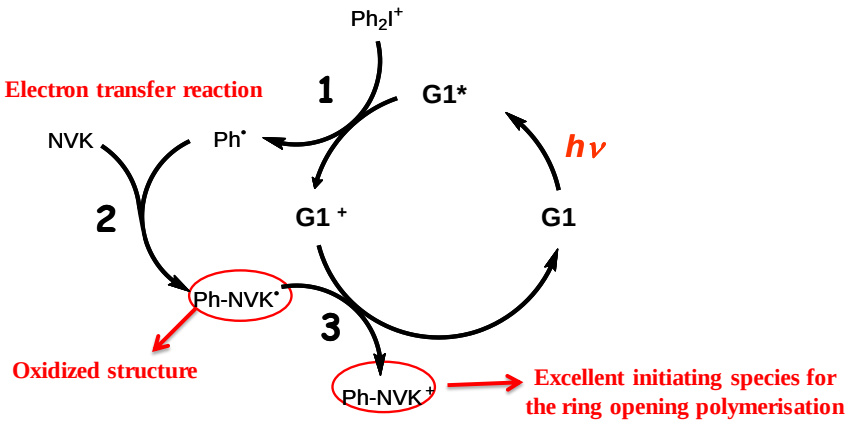

Figure 7. The proposed scheme for G1/Iod/NVK copper-complex (G1) photoredox catalyst systems for FRP and CP reported by Mokbel et al [29,30].

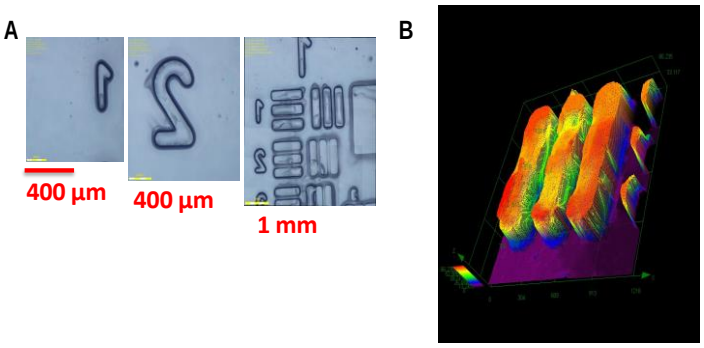

Figure 8. (A) 3D-photopolymerization experiments using LED projector @405 nm where the numbers and patterns can be easily observed by a numerical microscopy, (B) pattern characterized by profilometry [29].

2.6. Radical-mediated thiol-ene (TE) photopolymerizations

Radical-mediated thiol-ene (TE) photopolymerizations, as shown by Figure 9, exhibit the advantages of rapid and optically clear, excellent mechanical properties, exhibit delayed gelation, being relatively uninhibited by oxygen and enable radical polymerization of a wide range of thiol and vinyl functional group chemistries [14]. Depending on the specific ene selected, and exhibit reaction kinetics strongly dependent on the electronic density of the ene and the thiol-ene structures. However, competing vinyl homopropagation of the vinyl group, particularly for acrylates, is an undesirable side reaction in thiol–ene photopolymerizations [14].

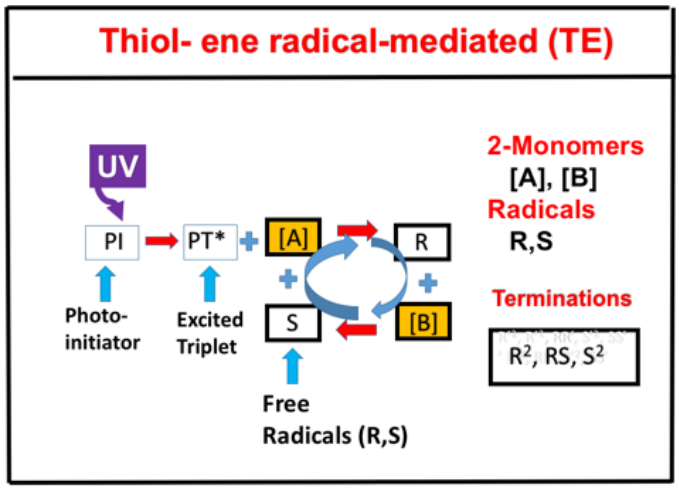

Figure 9. Schematics of thiol ([A]) and ene ([B]) functional groups, in which thiyl radical R reacts with [B], to form a carbon radical (S) which reacts with thiol and regenerates R to form the reaction cycle; R and S could interact with each other or terminated by bimolecular recombination. After Chen et al [14], Polymers 2019, 11, 1640; doi:10.3390/polym11101640.

Our numerical results for the conversion efficacy, C_T (for thiol [A]) and C_V (for ene [B]) show the roles of the reaction rate ratio, $R_K = k_P/k_{CT}$, and the concentration ratio, $R_C = [A]_0/[B]_0$ are consistent with our predicted results based on analytic formulas which provide more general features for the

roles of R_K and R_C, summarized as follows:

(i) Without the viscosity (with F=1) or homopolymerization (or k_{CV}=0) effects, [A] and [B] have an equal overall polymerization rate (R_P); C_V (C_T) is an increasing (decreasing) function of the ratio $R_C=[A]_0/[B]_0$. For R_K=1 (or $k_P=k_{CT}$), C_V and C_T have the same temporal profiles, but have a reversed dependence on R_C.

(ii) For $R_K<<1$, [B] and C_V are almost independent to R_C with a second-order correction proportional to R_C having asymmetric dependence on R_C given by (1-d), with d= R_K/R_C,

(iii) For $R_K>>1$, [A] and C_T are almost independent to R_C, but the second-order correction is inverse proportional to R_2,, an opposite trend in comparing with C_V. As predicted by analytic formulas.

(iv) With the presence of viscosity effect, the free-volume is reduced when crosslink efficacy increases. The reduction factor only affects the propagation rate constant, therefore, the viscosity effect affects does not affect the efficacy for the case of $R_K>>1$, and affects the efficacy for other ratios of k_P and k_{CT}, where the viscosity effect reduces the efficacy of [B].

(v) For optically-thick polymer, the influence of dynamic light intensity is due to PI depletion. Most previous modeling with a constant light intnesity the assumption suffers an error of 5% to 20% (underestimated) for a crosslink depth (Z_C) ranging 300 to 500 um.

(vi) Scaling law for the functional group concentration of thiol, [A], and ene, [B], given by $[A]^m[B]^n$. For $R_K>>1$, the polymerization rates are first order in ene concentration (or n=1.0) and nearly independent of the thiol concentration (or m=0); in contrast, m=1.0 and n=0 for $R_K<<1$. For R_K values near unity, polymerization rates are approximately 0.5 order in both thiol and ene functional group concentrations (m=n=0.5). However, a scaling law of m=0.4, and n=0.6 was found in an acrylate system (with R_K=13), due to contributions from homopolymerization [14].

2.7. Superbase Thiol–acrylate Michael (TM) addition and TE/TM systems

As show by Figure 10, TM addition reaction offers high modulus materials for applications such as coatings, dental restorative materials, shape memory materials, and composites [12,13]. It also has the unique potential for long-term dark-cure capability and insensitive to oxygen inhibition effects. Claudino et al [12] proposed a strategy of TM addition reaction using a superbase photogenerator as the initiation system involving a photobase UV-initiator, such as 2-(2-nitrophenyl)propyloxy- carbonyl-1,1,3,3-tetramethylguanidine (NPPOC-TMG) and coumarin-TMG, which have very low basicity and remain relatively stable within formulated monomer mixtures, but once photocleaved led to a dramatic increase in basicity of the released organobase. Claudino et al [12] also developed the modeling equations using two-step reaction mechanism for the catalytic cycle and predicted the overall kinetic behavior, where the fundamental phenomena, driving mechanisms and primary factors affecting TM are presented, but under certain assumptions. Lin at al (unpublished) further improve the proposed kinetics of Claudino et al [12] to include the vinyl group consumption by both propagation and the homopolymerization effect. Furthermore, Lin et al also include a diffusion factor counting for the decrease of kinetic constants due to the reduction of the free volume resulted from the increase of viscosity of the monomer and crosslinker molecules,

specially for the regime of high conversion efficacy. The light intensity, I(z,t), in the photoinitiation reaction was assumed as time and spatially independent by Claudino et al [12]. This assumption eliminates all the spatial profile information, and it is valid for an optically-thin samples and limited to small light dose.

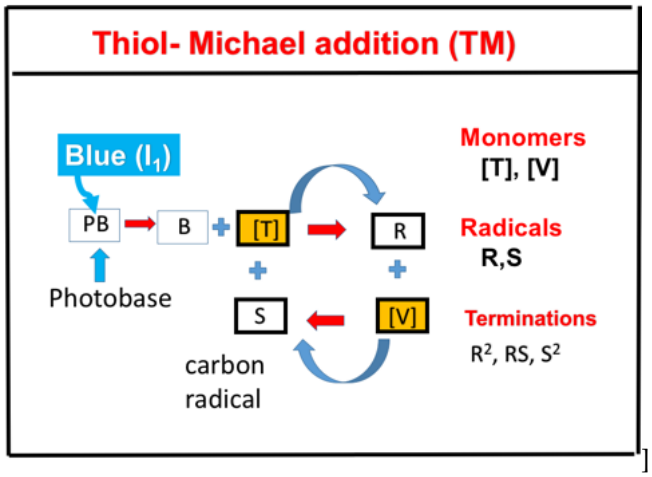

Figure 10. Kinetic scheme of a based-catalyzed thiol−Michael addition reaction with acid−base neutralization included as termination mechanism, shown by B+[HA]; Also included is the homopolymerization effect, shown by [C=C]+RC*. The reaction of deprotonations, propagation and chain-transfer are given by B+[SH], [C=C]+RS*, and [SH]+RC*, respectively. Notations used are: PB for the photobase catalyst, B for the photochemically yielded active-site base; [HB*], RS*, and RC* are intermediate reactive species for the conjugated acid, thiolate anion and thiocarbanion, respectively. [HA] is the initial acidic impurities related to the induction time and limits the availability of base catalyst for deprotonation. After Lin et al (unpublished).

Figure 11 shows the schematic for a combined TE and TM system under a dual-wavelength initiated mixture thiol ([T]), acrylates ([A], and methacrylates ([M] monomers. Notations used are: PB for the photobase catalyst, B for the photochemically yielded active-site base; PI is the initiator for TM, with triplet excited state PT*; R', R, S, S' are reactive species. After Lin et al (unpublished).

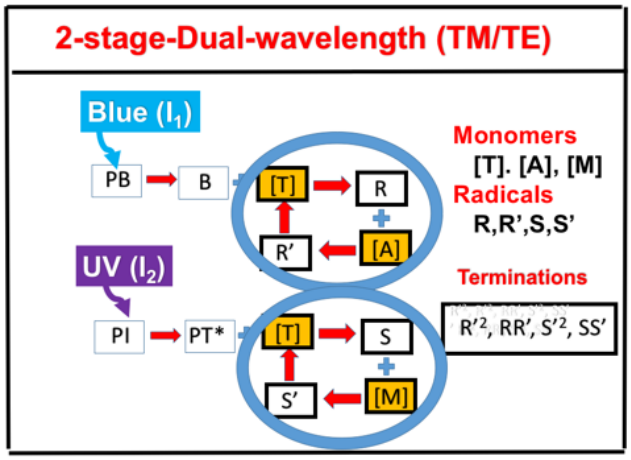

Figure 11. Kinetic scheme of a dual-wavelength initiated mixture of thiol ([T]), acrylates ([A], and methacrylates ([M] monomers; TM for based-catalyzed thiol−acrylate Michael addition reaction; and TE for thiol-methacrylate reaction; Notations used are: PB for the photobase catalyst, B for the photochemically yielded active-site base; PI is the initiator for TM, with triplet excited state PT*; R', R, S, S' are reactive species. After Lin et al (unpublished).

2.8. Dual-wavelength (UV and blue) controlled photopolymerization confinement (PC)

Variety of photoresponsive materials such as conjugated polymers have been reported for PC in AM and more recently for 3D and 4 D bioprinting [3-5]. Both spatial and temporal controlled 3D processes were reported using single and multiple wavelength lights. For 3D photo printings, Two stage polymerization under two wavelengths to eliminate the oxygen inhibition effects was also reported experimentally [9-11]. The advantages of dual-wavelength concurrent inhibition and initiation photopolymerization include: (i) controllable high vertical print speeds, (ii) eliminating the need for thin, oxygen-permeable projection windows, (iii) single-step fabrication of cured materials and (iv) rapid generation of personalized products. One additional advantage is that the reflow into the inhibition volume during printing can be optimized for large cross-sectional area parts.

Two different mechanisms of dual-wavelength selectively controlled photo-initiation and photo-inhabitation have been reported experimentally: (i) oxygen-inhibition reported by Childress et al [10]; and (ii) radical-inhibition reported by de Beer et al [8] and van der Laan et al [9]. In the first mechanism using red and UV light, the pre-irradiation time of red-light could be controlled to tailor the induction time, such that photosensitization and photoinitiation can be independently achieved for reduced oxygen inhibition for faster and more efficient UV-light polymerization. Figure 12 shows the schematics of photochemical dual wavelength (blue and UV) controlled volumetric 3D printing and AM for parallel lights and orthogonal lights patterns [8,9]. In the second mechanism, as shown by a proposed scheme in Figure 13 [21], in which the photochemical decomposition of butyl nitrite results in the formation of nitric oxide ([N]), an efficient inhibitor of radical-mediated polymerizations, and alkoxide radical (X) for extra polymerization initiation, beside the reactive radical (R). Concurrent with the blue-light photo-orthogonal, patterned irradiation, the blue-light produced initiation-radical could be reduced/inhibited by [N], such that photopolymerization confinement (PC) is achieved [18]. For PC application, large polymerization inhibition depth adjacent to the projection window, and continuous part production at high translation speeds are desired.

As reported by van der Laan et al. [11], the effectiveness of a photoinhibitor is strongly monomer-dependent, which also requires: (i) a high conversion of blue-photoinitiation in the absence of the UV-active inhibitor; (ii) a strong chain termination with significant reduction of blue and UV conversion in the presence of UV-active inhibitor and (iii) short induction time or rapid elimination of the inhibitor species in the dark (or absence of UV-light), such that the initiation–inhibition cycles may be switched on and off rapidly. Fast switching-time may be achieved by high conversion rate, or high blue-light intensity,

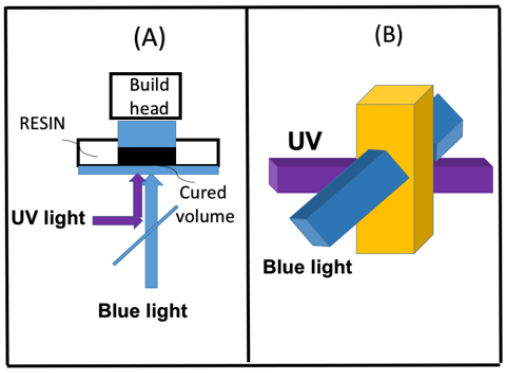

Figure 12 shows the schematics of photochemical dual wavelength (blue and UV) controlled volumetric 3D printing and additive manufacturing (AM) for parallel lights and orthogonal lights patterns [8,9].

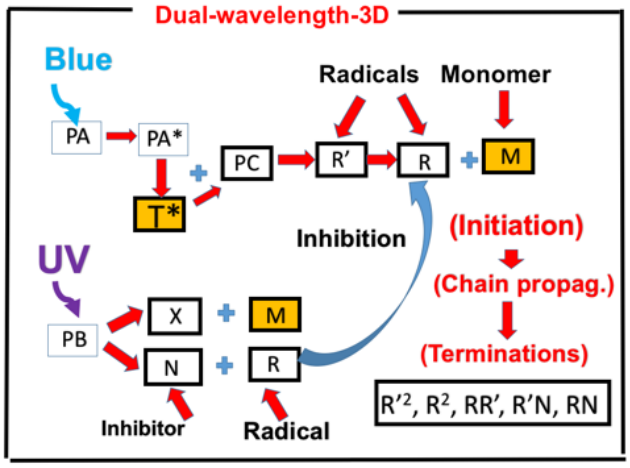

Figure 13. Schematics of photochemical pathways of dual wavelength photopolymerization; in which crosslinkers are formed via two pathways, via the photoinitiator PA (under a blue light), and PB (under a UV light). The initiation radicals R and [X] crosslink with the monomer [M]; whereas the inhibition radicals [N] reduces the conversion efficacy by reducing the active radicals (R' and R). Shown also is the co-initiator (PC), which reacts with the triplet state of PA (T*) forming an intermediate radical (R'). Bimolecular termination of R' produces a propagating radical (R) which leads to crosslinks; terminations could be also resulted by the interaction of R and R', and R and [N]. After Lin et al [21], Polymers, 2019, 11, 1819.

2.9. Dual-wavelength (UV and red) controlled 3D printing

There are many conventional strategies to reduce oxygen inhibition in photoinduced polymerizations. Physical methods include: working in an inert or closed environment, increasing the photoinitiator concentration, increasing the light dose, or light intensity (for reduced induction time), use of multiple photoinitiators with different rate of initiation, or addition of oxygen scavengers. Chemical mechanisms incorporate additives or suitably functionalized monomers which are insensitive to oxygen, such as the TE and TM additive systems [12,14]. To overcome oxygen inhibition, phthalocyanines were explored as with a relatively long triplet state lifetime (5 to 350 micro-second) and a high quantum yield (0,58-0.65).

Figure 14 shows the schematics of photochemical for red-light, oxygen-mediated (type-II) and UV-light, radical-mediated (type-I) pathway [19]. The strategies for controlled initiation-inhibition switch based on two mechanisms: (i) oxygen-inhibition for improved conversion, and (ii) radical-inhibition for spatial confirmation in 3D printing. Example of Figure 14 kinetics was reported by

Childress et al [11], based on a of ethyl ether acrylate (DEGEEA) mixed by zinc 2,9,16,23-tetra-tert-butyl-29H,31H-phthalocyanine (ZnTTP), having distinct absorption peak at UV-365 nm and red-635 nm, such that it can be independently excited by a UV and red light, respectively.

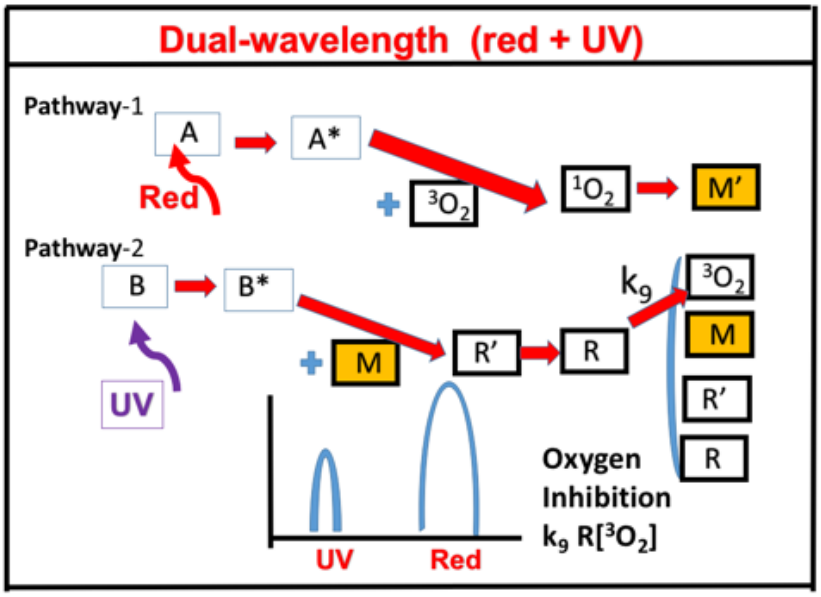

Figure 14. Schematics of photochemical for pathway-1, red-light, oxygen-mediated (type-II) and pathway-2, UV-light, radical-mediated (type-I); where A and B are the ground state photosensitizer (PS) and photoinitiator (PI), having triplet excited state A* and B* and free radicals R' and R; $^3O_2$ and $^1O_2$ are the ground state and singlet oxygen; M' and M are the monomers. Also shown is the absorption spectra with peaks at UV (365 nm) and red (635 nm). After Lin et al [19], J Polymer Science, 2020, 58, 683-691.

2.10. Three-wavelength controlled in 3D printing and additive manufacturing (AM).

Figure 15 shows the schematics of three photochemical pathways of a 3-wavelength photopolymerization [22]: (i) the photoinitiator A (under a blue light), (ii) B (under a UV light), and (iii) oxygen-mediated C (under a red light). Higher oxygen concentration leads to a lower conversion, which could be enhanced by reducing the S-inhibition via a red or blue light pre-irradiation. We found that pre-irradiation time is given by $T_P = 200$ s for red-light only, and reduced to 150 s, for both red and blue-light. The system under UV-only leads to a conversion lower than that of blue-only. However, conversion could be improved by the dual-light (blue and UV), and further enhanced by the pre-irradiation of red-light. The two competing factors, N-inhibition and S-inhibition, could be independently and selectively tailored to achieve: (i) high conversion of blue-light (without UV-light), enhanced by red-light pre-irradiation for minimal S-inhibition; and (ii) efficient PC initiated by UV-light produced N-inhibition for reduced confinement thickness and for high print speed.

The red-blue-UV system could be extended to the following as far as these 3 wavelengths have minimal overlap in their absorbance spectra, such as: (i) red-light (635 nm), green (532 nm), and UV-A (365 nm); (ii) near-IR (750-810 nm), red (630-660 nm), and near UV (365-405 nm); where most of these lights are available from the output of LED, and the associated photosensitizers (or photoinitiator).

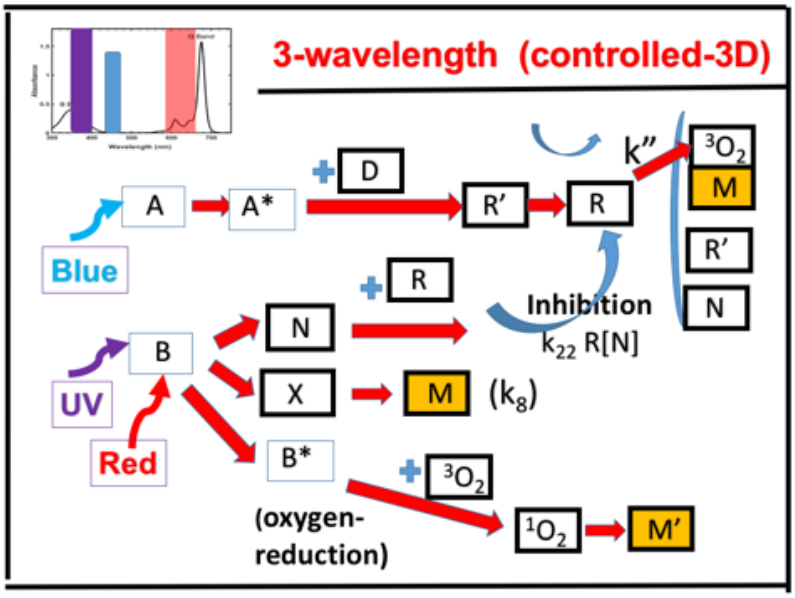

Figure 15. Schematics of photochemical pathways of a 3-wavelength photopolymerization, in which crosslinkers are formed via three pathways: the photoinitiator A (under a blue light), B (under a UV light), and oxygen-mediated C (under a red light). The initiation radicals R, [$^1O_2$] and [X] initiate the monomer [M] polymerization; whereas the inhibition radical [N] reduces the active radical R. Also shown is the co-initiator (D) which reacts with the triplet state of A (A*) forming an intermediate radical (R') and a reactive radical (R), initiating crosslinkers; terminations may be resulted by the interaction among R', R and [N]. After Lin et al [22], IEEE Access, 2020, 8, 49353-49362.

3. Formulas and Results

We will present the basic formulas associate t the photopolymerization conversion and soem key parameters for 3 D printing and AM. Dynmaic profiles numerically produced will be shown for selected systems with comparison to measured data. Greater details and more complex formulas can be found in the Refrences cited.

3.1. Basic formulas for conversion and rate functions

For a single initiator [A] system with bimolecular terminationand in thenpresentce of oxygen O_2, the free radical concentration is given by $R=([A]/ k_T)^{0.5} – K_{12}[O_2]$, which is a decreasing function of oxygen [32]. Using the quasi-steady-state conditions, the monomer conversion is given by

$$\frac{\partial[\mathbf{M}]}{\partial \mathbf{t}} = -\mathbf{R_T}[\mathbf{M}] \quad (1)$$

$$\mathbf{R_T(t)} = \mathbf{k'}\sqrt{\mathbf{0.5bI(z,t)[A]/k_T}} - \mathbf{K_{12}[O_2]} \quad (2)$$

where I(z,t) is the light intensity, and b is a coupling constant.

The FRP conversion efficacy is given by $C_V=1- \exp(-S)$, with the S-function given by the time integrate of the rate function R_T. For a type-I dominated mechanism with ignored oxygen effects, the S function is given by [32]

$$\mathbf{S} = \mathbf{KG(z,t)}\sqrt{\mathbf{bI_0X[A]_0}} \quad (3)$$

$$\mathbf{G(z,t)} = [\mathbf{1} - \mathbf{exp}\,[-\mathbf{0.5B't}]]/\mathbf{B'} \quad (4)$$

where $K=k'/k_T^{0.5}$, $B'=bI_0X$, $X=\exp[-A_2z]$, with $A_2=2.3(a'[A]_0+q')$.

Eq. (3) shows that the conversion is proportional to $B'^{0.5}t$, for transient state (small t), but it is proportional to $B'^{-0.5}$ for steady state.

3.2. *Basic formulas for 3D printing*

For dual-wavelength (UV and blue) controlled photopolymerization confinement (PC). The maximum print speed (Smax) as defined by de Beer et al. [9], when the dose difference of blue light and UV light equals to a critical value (E*), and $B_1 = \boldsymbol{\beta} B_2$, we obtain a similar formula:

$$\mathbf{S_{max}} = \frac{\mathbf{B_{20} - \beta B_{10}}}{\mathbf{E^*}}, \qquad (5)$$

where $B_{j0} = b_j I_{j0}(z,t)$, $\beta = (C_2 b_{20}/b_{10})/(g C_1 C_3)$, Cj (with j-1,2,3) are the concentration of the 3 co-initiators, I_{j0}, (with j=1,2) the UV and blue light intensity and b_{j0} are coupling constant. The simplified function of de Beer et al. [9] is when $\beta = b_{20}/b_{10}$.

Curing depth and Inhibition zone are the critical parameters for 3D printing and AM. A curing depth (Z_C) is defined by when the conversion efficacy is higher than a critical value, $C_{EFF} > C_T$, or when $S > S_T$, with $S_T = \ln [1/(1-C_T)]$. Using Equation (3), and let $S = S_T = 2$ (or $C_T = 0.86$), Z_C is related to the crosslink time (T_C) by

$$\mathbf{T_C} = \left(\frac{\mathbf{1}}{\mathbf{B''}}\right) \mathbf{ln}[\mathbf{2B'}/(\mathbf{K'}\sqrt{\mathbf{0.5bXI_0[A]_0}}) - \mathbf{1}] \qquad (6)$$

The above curing depth (Z_C) is proportional to the pillar height measured in AM [10].

3.3. Conversion profiles

We will show selected temporal profiles (numerically produced) for various systems at follows. Figure 16 and 17 show the dynamic profiles (in dual initiators system) of oxygen and the conversion at various light intensity. in which higher light intensity leads to faster oxygen depletion and higher efficacy [41]. Figure 18. Conversion profiles in an enhancer [B} system, in which higher concentration $[B]_0$ leads to faster and higher conversion [41]. Figure 19 shows the conversion profiles for CQ/DMABN/AY system, in which higher initiator concentration of CQ leads to higher conversion. Figure 20 and 21 show the CP profiles of epoxy functions of the model resin in air in the presence of curve-1 for 2-ITX/Iod (0.25/4.3 %w/w), curve-2 for Anthracene/Iod (0.23/4.8 %w/w), and curve-3 G1/Iod/NVK, demonstrating that G1 (copper complex) is the most efficient initiator [29, 30]. Figure 22. shows the methacrylate conversion of a bisGMA/TEGMA resin formulated with 0.2wt%CQ/0.5wt%EDAB/0.5 wt% BN and subject to a continuous exposure of a blue light, but an on-off exposure of a UV-light, serving as an optical-switch [10,21]. Figure 23 shows that higher red-light pre-irradiation time or light dose leads to a lower induction time for a fixed red-light intensity, in a 3D or AM systems. [10].

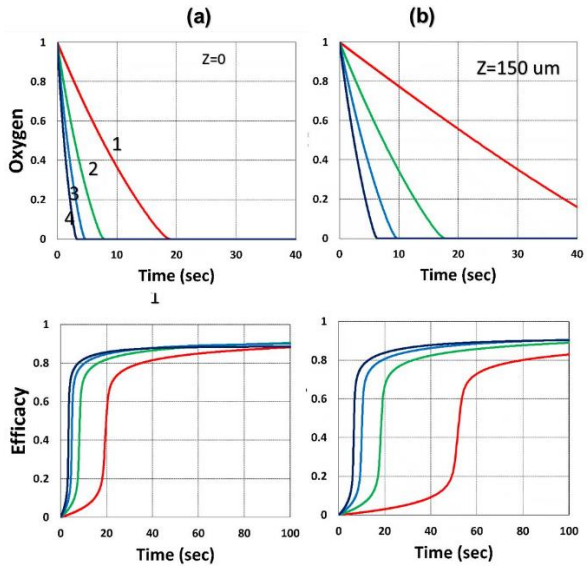

Figure 16 Dynamic profiles of oxygen and the conversion at various light intensity I_0=(0.5,2,5,10) mW/cm^2, for curves (1,2,3,4); at z=0 (left, on surface) and 150 um (right) [41].

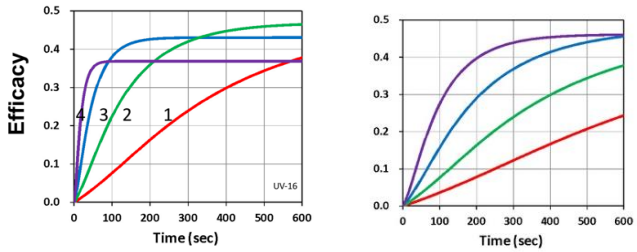

Figure 17. UV-light initiated conversion efficacy but for (left Figure), b_2=(0.05, 0.08, 0.11, 0.14), for curve (1,2,3,4); and for (right Figure) I_{20} =(10, 20,40,80) mW/cm^2. [41]

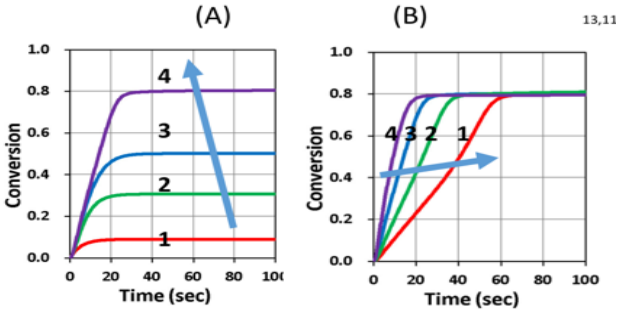

Figure 18. Conversion profiles in an enhancer system: (A) concentration $[B]_0$ = (0,0.5,1.0,2.0) %, for curve (1,2,3,4); with $[A]_0$=3.0%, $[C]_0$=0.1%, b'=bI_0 = 0.6 (1/s/%); and (B) coupling constant b'=bI_0 = (0.15,0.3,0.6,1.2) (1/s/%), with $[A]_0$=3.0%, $[B]_0$=2.0%, $[C]_0$=0.1%, $[O_2]_0$=1.5mg/L; and k'=0.7, k''=2.5, k_T=k_2=2.0, k_1=0.7, k_3=8, k_5= k_7=1 (1/s). After Chui et al [18].

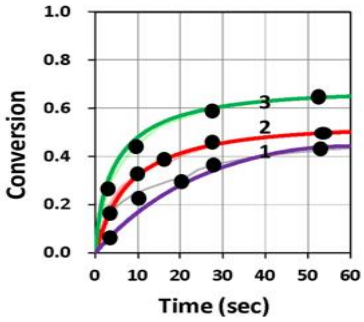

Figure 19. Conversion profiles for CQ/DMABN/AY (1.5/0.6/0.75 % w/w) system; curve-1 without AY (or A_0=0), and curve 2 and 3 for A_0=0.2 and 0.75% with B_0=0.6% and C_0=1.5%. Dots are measured data of Kirschner et al[15], and solid curves are fit modeling curves of Lin et al [20].

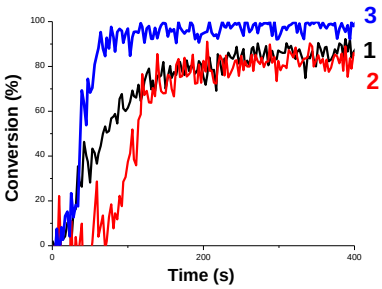

Figure 20. Photopolymerization profiles of epoxy functions of the model resin in air in the presence of (1) 2-ITX/Iod (0.25/4.3 %w/w), (2) Anthracene/Iod (0.23/4.8 %w/w), and (3) G1/Iod/NVK (0.22/5/1 %w/w/w), upon LED@405 nm exposure, sample thickness = 1.4 mm. After Mokbel et al [29]

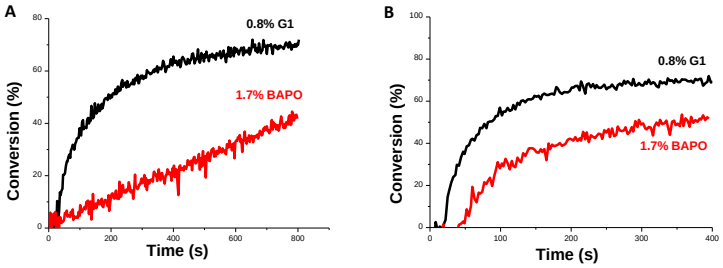

Figure 21. Photopolymerization profiles (epoxy function conversion vs. irradiation time) for DGEBA in air in the presence of G1/Iod/NVK (0.8/4.6/1 %w/w/w) or BAPO/Iod/NVK. After Mokbel et al [29].

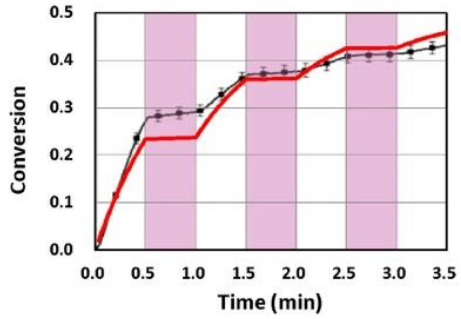

Figure 22. Methacrylate conversion of a bisGMA/TEGMA resin formulated with 0.2wt%CQ/0.5wt%EDAB/0.5 wt% BN and subject to a continuous exposure of a blue light, but an on-off exposure of a UV-light for 0.5 minute, as indicated by the violet vertical araes; where black bars are measured data from van der Laan et al. [10] and red curve is theoretical simulation of Lin et al [21].

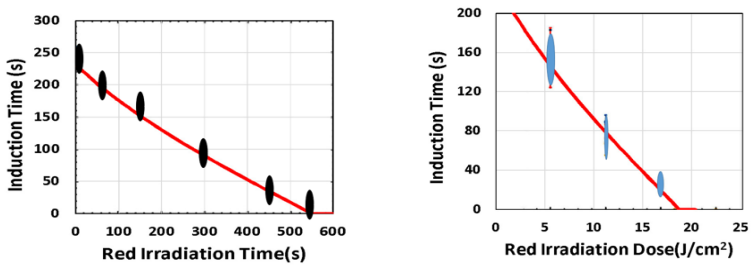

Figure 23. Induction time (T_{ID}) versus red-light pre-irradiation time (T_P) (left Figure) for a fixed I_{10} (red)= 34 mW/cm² and I_{20}(UV)=10 mW/cm²; and (right Figure) for T_{ID} vs. red-light dose for I_{10} (red)= (10,20,30) mW/cm². Red curves are modeling data by Lin et al [19], also shown are the measured data (in bars) of Childress et al [10].

4. Conclusion

As shown in Table 1, we have reviewed the important topics which were recently reported or proposed to conduct. Various modelings and kinetic schemes are proposed theoretically and compared with specfic reported measurements. We conclude the following important features.

(i) CXL using UVA (365 nm) and riboflavin solution as the initiator (photosensitizer) has type-I and type-II FRP pathwyas. agent). Oxygen plays an important role, specially for type-II, in which oxygen singlet radical has been used to kill cancer cells.

(ii) Synergic effects are achieved by a dual-function enhancer, in which the FRP is improved by the reduction of oxygen inhibition effects. The reported measurement system [17] is a 3-component system of C/B/A, in which [C]= IR-140 borate, [B] = 4-(Diphenylphosphino) benzoic acid (4-dppba), and [A] = iodonium salt $Ar_2I+PF_6^-$, with initial concentration of [0.1/2.0/3.0] wt%, and mixed in a monomer [M]=methacrylate.

(iii) Synergic effects are achieved by a 3-initiator system, having two pathways of electron-transfer and oxygen-mediated energy-transfer, in which the presence of amine produces additional initiating radicals and hence improve the FRP. The reported measurement system is (CQ)/amine/AY system of Kirschner et al. [15], in which higher AY (from 0% to 0.75%) leads to higher conversion (from about 40% to 60%).

(iv) The reported measurement system [29] was copper-complex (G1) photoredox catalyst in G1/Iod/NVK systems for FRP and CP, in which the co-initiators/additives Iod and NVK have dual functions of: (i) regeneration of photoinitiator and (ii) generation of extra radicals. The synergic effects lead to higher conversion of FRP and CP.

(v) Radical-mediated thiol-ene (TE) photopolymerizations. It offers advantages of rapid and optically clear, exhibit delayed gelation and relatively uninhibited by oxygen for efficient FRP.

(vi) Superbase photogenerator based-catalyzed thiol–acrylate Michael (TM) addition reaction. It has the unique potential for long-term dark-cure capability and insensitive to oxygen inhibition effects. A dual-wavelength combined system of TE and TM could offer very efficient conversion with controlled profiles.

(vii) Dual-wavelength (UV and blue) system was reported for controlled photopolymerization confinement (PC) for volumetric 3D printing and AM using parallel lights and orthogonal lights patterns [11].

(viii) Dual-wavelength (UV and red) selectively controlled 3D printing, in which red-light pre-irradiation improves the conversion [9,19].

(ix) 3-wavelength system is proposed for controlled 3D printing and AM, in which the two competing factors: N-inhibition and S-inhibition, could be independently and selectively tailored to achieve: (i) high conversion of blue-light (without UV-light), enhanced by red-light pre-irradiation for minimal S-inhibition; and (ii) efficient PC initiated by UV-light produced N-inhibition for reduced confinement thickness and for high print speed.

To conclude, with minimum mathematics, we present (for the first time), the synergic features and enhancing strategies for various systems of multi-commponents, initiators, monomers, and under one- two- and there-wavelength light. Therefore, this Review provides not only the bridging of modeling and measurements, but also guidances for further experimantal stuides and new applications in 3D printings and AM, based on the innovative concepts (kinetics/schemes).

Funding: The Agence Nationale de la Recherche (ANR agency) is acknowledged for its financial support through the NoPerox grant.

Acknowledgments: JTL thanks the internal grant of New Vision Inc. and DCC thanks the financial support from 359 China Medical University with the grant number CMU109-S-39.

Conflicts of Interest: Jui-Teng Lin is the CEO of New Vision Inc.

References

1. Fouassier, J. P. & Lalevée, J. Photoinitiators for Polymer Synthesis-Scope, Reactivity and Efficiency. Wiley-VCH Verlag GmbH & Co. KGaA: Weinheim, Germany, 2012.
2. Yagci, Y., Jockusch, S. Turro, N.J. Photoinitiated polymerization: Advances, challenges and opportunities. *Macromolecules* **43**, 6245–660 (2010).
3. Ligon, S.C.; Liska, R.; Stampfl, J.; Gurr, M et al. Polymers for 3D printing and customized additive manufacturing. *Chem. Rev.* **2017**, *117*, 10212−10290.
4. Takagishi, K.; Umezu, S. Development of the improving process for the 3D printed structure. *Sci. Rep.* **2017**, *7*, 39852.
5. Shusteff, M.; Browar, A.E.M.; Kelly, B.E.; Henriksson, J et al. One-step Volumetric Additive Manufacturing of Complex Polymer Structures. *Sci. Adv.* **2017**, *3*, 7.

6. Janusziewicz, R.; Tumbleston, J.R.; Quintanilla, A.L.; Mecham, S.J. et al. Fabrication with Continuous Liquid Interface Production. *Proc. Natl. Acad. Sci. USA* **2016**, *113*, 11703−11708.
7. Kelly, B.E.; Bhattacharya, I.; Heidari, H. et al, Volumetric Additive Manufacturing via Tomographic Reconstruction. *Science* **2019**, *363*, 1075−1079.
8. de Beer, M.P.; van der Laan, H.L.; Cole, M.A. et al. Rapid, Continuous Additive Manufacturing by Volumetric Polymerization Inhibition Patterning. *Sci. Adv.* **2019**, *5*, 8.
9. van der Laan, H.L.; Burns, M.A.; Scott, T.F. Volumetric Photopolymerization Confinement through Dual-Wavelength Photoinitiation and Photoinhibition. *ACS Macro Lett.* **2019**, *8*, 899–904.
10. Childress, K.K.; Kim, K.; Glugla, D.J. et al. Independent control of singlet oxygen and radical generation via irradiation of a two-color photosensitive molecule. Macromolecules **52**(13):4968–4978 (2019).
11. Scott, T.F.; Kowalski, B.A.; Sullivan, A.C. et al. Two-Color Single-Photon Photoinitiation and Photoinhibition for Subdiffraction Photolithography. *Science* **2009**, *324*, 913–917.
12. Claudino,M.; Zhang,X.; Alim,M.D. et al. Mechanistic Kinetic Modeling of Thiol-Michael Addition Photopolymerizations via Photocaged "superbase" Generators: An Analytical Approach. Macromolecules 2016, 49 (21), 8061−8074.
13. Huang, S.; Sinha, J.; Podgorski, M. et al. Mechanistic modeling of the Thiol−Michael addition polymerization kinetics: Structural effects of the Thiol and Vinyl monomers. *Macromolecules* **2018**, *51*, 5979–5988.
14. Chen, K.T., Cheng, D.C., Lin, J.T. Liu, H.W. Thiol-Ene photopolymerization in thick polymers: kinetics and analytic formulas for the efficacy and crosslink depth. *Polymers* **11**, 1640 (2019) doi:10.3390/polym11101640.
15. Kirschner, J., Paillard, J., Bouzrati-Zerell, M, et al. Aryliodonium ylides as novel and efficient additives for radical chemistry: example in camphorquinone (CQ)/Amine based photoinitiating systems. *Molecules* **24**(16), 2913 (2019); doi:10.3390/molecules24162913.
16. Schmitz C, Halbhuber A, Keil D, Strehmel B. NIR-sensitized photoinitiated radical polymerization and proton generation with cyanines and LED arrays. Prog. Org. Coat. 2016, 100, 32−46.
17. Bonardi AH, Dumur F, Grant TM, et al. High performance near-Infrared (NIR) photoinitiating systems operating under low light intensity and in the presence of oxygen. Macromolecules, 2018, 51, 1314-1324.
18. Chiu YC, Cheng DC, Lin JT, Chen KT, Liu HW. Dual-function enhancer for near-infrared photopolymerization: kinetic modeling for improved efficacy by suppressed oxygen inhibition. IEEE Access, 2020, 8, 83465-83471.
19. Lin JT, Liu HW. Chen KT, Chiu YC, Cheng DC. Enhancing UV photopolymerization by a red-light pre-irradiation: kinetics and modeling strategies for reduced oxygen-inhibition. J Polymer Science, 2020，58， 683-691，DOI:10.1002/pol.20190201.

20. Lin JT, Chen KT, Chang PK, Cheng DC. Enhancing blue-light-initiated photopolymerization in a three-component system: kinetic and modeling of conversion strategies. **J** Polymer Research, 2021, 28:2.
21. Lin JT, Chen KT, Cheng DC, Liu HW. Dual-wavelength (UV and blue) controlled photopolymerization confinement for 3D-printing: modeling and analysis of measurements. Polymers, 2019, 11, 1819.
22. Lin, J.T., Liu, H.W., Chen, K.T. Cheng, D.C. 3-wavelength (UV, blue, red) controlled photopolymerization: improved conversion and confinement in 3D-printing. IEEE Access, 2020, 8, 49353-49362.
23. Liu, S.; Chen, H.; Zhang, Y.; Sun, K.; et al. Monocomponent photoinitiators based on Benzophenone-carbazole structure for LED photoinitiating systems and application on 3D printing. Polymers, 2020, *12*(6), 1394.
24. Chen KT, Lin JT, Liu HW. Enhancing Radical-mediated Photopylomerization Efficacy and Crosslink Depth: Kinetic and Model of a Two-monomer System. Res Med Eng Sci. 2019, 8(2):853-860.
25. Abdallah, M.; Dumur,F.; Graff, G.; et al High performance dyes based on triphenylamine, cinnamaldehyde and indane-1,3-dione derivatives for blue light induced polymerization for 3D printing and photocomposites. Dyes and Pigments, **182**, 108580 (2020).DOI: 10.1016/j.dyepig.2020.108580.
26. Abdallah, A.; Hijazi,A.; Lin, J.T.; Graff, B.; Dumur, F.; Lalevee, J. Coumarin Derivatives as Photoinitiators in Photo-Oxidation and Photo-Reduction Processes and a Kinetic Model for Simulations of the Associated Polymerization Profiles. App Polymer Material. 2020, 2,2769-2780.
27. Sun, K.; Liu, S.; Pigot , C.; et al Novel Push–Pull Dyes Derived from 1H-cyclopenta[b]naphthalene-1,3(2H)-dione as Versatile Photoinitiators for Photopolymerization and Their Related Applications: 3D Printing and Fabrication of Photocomposites. Catalysts, **10**, 1196 (2020). DOI: 10.3390/catal10101196
28. Mokbel, H.; Anderson, D.; Plenderleith, R.; Dietlin, C.; et al. Copper photoredox catalyst "G1": A new high performance photoinitiator for near-UV and visible LEDs. *J. Polym. Chem*. **2017**, *8*, 5580–5592.
29. Mokbel, H.; Anderson, D.; Plenderleith, R.; Dietlin, C.; et al. Simultaneous initiation of radical and cationic polymerization reactions using the "G1" copper complex as photoredox catalyst: Applications of free radical/cationic hybrid photopolymerization in the composites and 3D printingfields. Prog. Org. Coat., **132**, 50–61 (2019). DOI: 10.1016/j.porgcoat.2019.02.044
30. Lin, J.T.; Lalevee, J.; Cheng, D.C. Kinetics analysis of copper complex photoredox catalyst: roles of oxygen, thickness, and optimal concentration for radical/cationic hybrid photopolymerization. Polymers (2021, in press),
31. Wertheimer CM, Elhardt C, Kaminsky SM et al. Enhancing rose Bengal photosensitized protein crosslinking in the cornea. Invest. Ophthalmol Vis Sci. 2019, 60, 1845-1852.

32. Lin, J.T,; Cheng, D.C. Modeling the efficacy profiles of UV-light activated corneal collagen crosslinking. PloS One. 2017;12:e0175002.
33. Lin JT. Photochemical Kinetic modeling for oxygen-enhanced UV-light-activated corneal collagen crosslinking. Ophthalmology Research, 2017;7:1-8.
34. Lin JT. Efficacy S-formula and kinetics of oxygen-mediated (type-II) and non-oxygen-mediated (type-I) corneal cross-linking. Ophthalmology Research. 2018; 8(1): 1-11.
35. Lin JT, Chiang S, Lin GH, Liu HW. In vitro photothermal destruction of cancer cells using gold nanorods and pulsed-train near-infrared lase. J. Nanomaterials. 2012; article ID 861385.
36. Lin JT, Chen KT, HW Liu. Analysis of kinetics and efficacy of anti-cancer via oxygen-enhanced photodynamic therapy. J Cancer Research update, 2018, 7:21-23.
37. Zhu TC, Finlay JC, Zhou X, et al. Macroscopic modeling of the singlet oxygen production during PDT. Proc SPIE 6427 (2007):6427O81– 6427O812.
38. Lin JT. Advances of Cancer Synergic Photo-Therapy: Kinetics and Efficacy. Nov Appro in Can Study. 2(1). NACS.000529.2018. DOI: 10.31031/NACS.2018.02.000529.
39. Kim JY, Choi W, Kim M, Tae G. Tumor-targeting nanogel that can function independently for both photodynamic and photothermal therapy and its synergy from the procedure of PDT followed by PTT. Journal of Controlled Release; 2013; 171:113–121.
40. Wang YH, Chen SP, Liao AH et al. Synergic delivery of gold nanorods using multifunctional microsbubbles for enhanced plasmonic photothermal therapy. Scientific Report. 2014: 5685. doi:10.1038/srep0585.
41. Lin JT, Chen KT, Cheng DC, Liu HW. Modeling the efficacy of radical-mediated photopolymerization: the role of oxygen inhibition, viscosity and induction time. Front. Chem.2019, 7:760. doi: 10.3389/fchem.2019.00760.